



# Preparation, characterization, and electrochemical application of mesoporous copper oxide

Liang Cheng<sup>a,b</sup>, Mingwang Shao<sup>a,b,\*</sup>, Dayan Chen<sup>b</sup>, Yuzhong Zhang<sup>b</sup>

<sup>a</sup> Functional Nano & Soft Materials Laboratory (FUNSOM), Soochow University, Suzhou 215123, PR China

<sup>b</sup> Anhui Key Laboratory of Functional Molecular Solids, and College of Chemistry and Materials Science, Anhui Normal University, Wuhu 241000, PR China

## ARTICLE INFO

### Article history:

Received 21 May 2008

Received in revised form 30 May 2009

Accepted 3 August 2009

Available online 8 August 2009

### Keywords:

A. Oxides

B. Chemical synthesis

D. Electrochemical properties

## ABSTRACT

Mesoporous CuO was successfully synthesized via thermal decomposition of  $\text{CuC}_2\text{O}_4$  precursors. These products had ring-like morphology, which was made up of nanoparticles with the average diameter of 40 nm. The electrochemical experiments showed that the mesoporous CuO decreased the overvoltage of the electrode and increased electron transference in the measurement of dopamine.

© 2009 Elsevier Ltd. All rights reserved.

## 1. Introduction

Mesoporous materials, which have excellent catalytic [1,2], electrical [3], and surface properties [4], have been focused on in various fields. And numerous preparation methods have been proposed, such as, sol–gel techniques [5], hydrolysis processes [6], polyglycol-assisted routes [4], inorganic and organic templates [7,8], ultrasonic ways [9], and co-precipitation approaches [10].

Among the various materials, copper oxide (CuO), as an important *p*-type transition-metal oxide with a narrow band gap ( $E_g = 1.2$  eV), has attracted much attention due to its photochemical and photoconductive properties [11,12], and excellent catalytic activity [13–15].

In this work, copper oxalate template method was chosen, because metal oxalates can be transformed to oxides or metals without losing the ordered structure [16]. And numerous works on the structure, properties and thermal behavior of metal oxalates have been published [17–19]. Copper oxalate is a material with polymer-like structure described as a stacking of  $\text{Cu}(\text{C}_2\text{O}_4)$ - $\text{Cu}(\text{C}_2\text{O}_4)$  ribbons [20]. The cushion- and rod-like shapes of copper oxalate had been produced via a precipitation reaction, and a brick-by-brick growth mechanism was proposed by Bowen and coworkers [21].

Herein, we synthesized ring-like copper oxalate in large scale via a simple reflux method, and further successfully prepared mesoporous CuO composed of nanoparticles with average diameter of 40 nm by thermal decomposition of copper oxalate. The optical and electrical properties of the CuO materials were investigated.

## 2. Experiment

### 2.1. Synthesis of $\text{CuC}_2\text{O}_4$ and CuO nanostructures

All the reagents in the experiments were analytically pure, purchased from Shanghai Chemical Company, and used without further purification. In a typical procedure, 20 ml  $\text{Na}_2\text{C}_2\text{O}_4$  (0.02 M) was dropwise added into 20 ml  $\text{CuSO}_4 \cdot 5\text{H}_2\text{O}$  (0.02 M) aqueous solution under magnetic stirring. Then the suspension was transferred to a round-bottom flask, refluxed at 100 °C for 2 h, and cooled to room temperature. The resultant was collected, and washed several times with absolute ethanol and distilled water, and dried under vacuum at 65 °C for 5 h. Finally the obtained copper oxalate precursors were heated to 400 °C at a ramping rate of 10 °C  $\text{min}^{-1}$  and calcined at 400 °C for 5 h to give copper oxide products.

### 2.2. Characterization

The phase and crystallography of the products were characterized by a Shimadzu XRD-6000 X-ray diffractometer equipped with Cu  $K\alpha$  radiation ( $\lambda = 0.15406$  nm). A scanning rate of 0.05  $\text{s}^{-1}$  was applied to record the pattern in the  $2\theta$  range of 20–70°. The

\* Corresponding author at: Functional Nano & Soft Materials Laboratory (FUNSOM), Soochow University, Suzhou 215123, PR China.  
Tel.: +86 512 65880953; fax: +86 512 65882846.

E-mail address: [mwshao@suda.edu.cn](mailto:mwshao@suda.edu.cn) (M. Shao).

morphologies of copper oxalate and copper oxide were analyzed with an S-4800 field emitting scanning electron microscopy (FESEM). TG-DTA measurement of copper oxalate was performed in SETARAM-TGA92 in the temperature range from room temperature to 400 °C at a heating rate of 10 °C min<sup>-1</sup>. The pore-size and distribution was measured on a Micrometrics ASAP-2000 adsorption apparatus.

### 2.3. The properties of the products

The optical property of the products was investigated by a UV–vis spectrophotometer (Shimadzu U-4100). A small amount of the sample was dispersed in ethanol for UV–vis absorbance spectroscopy measurement in the wavelength range between 200 and 800 nm.

Electrochemical experiments were performed with electrochemistry work station (CHI 620B, ChenHua Instruments Co.) with a conventional three-electrode system. A saturated calomel electrode (SCE) and a platinum wire were employed as the reference electrode and the counter electrode, respectively. The CuO/GCE was used as working electrode, which was fabricated as follows: mesoporous CuO powder (0.01 g) was added in 5 ml *N,N*-dimethylformamide (DMF) under ultrasonic irradiation to get CuO suspension. GCE ( $\Phi = 2$  mm) was polished with 0.05  $\mu$ m alumina slurry and washed with 1:1 nitric acid, ethanol and water in an ultrasonic bath for a few minutes. After washing with sonication, the GCE was coated with 10  $\mu$ l CuO suspension, and dried at room temperature.

## 3. Results and discussion

Fig. 1a is the XRD pattern of the resultants after refluxing. All the diffraction peaks may be indexed as orthorhombic phase copper oxalate (JCPDS No. 21-0297). Fig. 1b displays the XRD pattern of CuO, obtained by calcining at 400 °C for 5 h. No other characteristic peaks were observed except for those for CuO (JCPDS No. 41-0254), indicating the as-obtained products has high-purity.

Fig. 2a and b shows the FESEM images of ring-like Cu<sub>2</sub>O<sub>4</sub> under low and high magnification, respectively. The low magnification

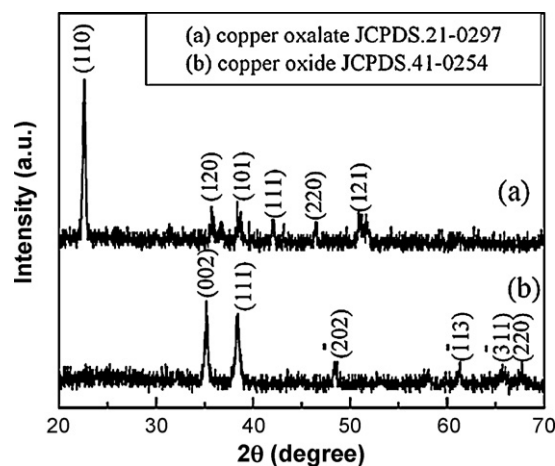


Fig. 1. XRD patterns of: (a) copper oxalate and (b) copper oxide.

SEM image (Fig. 2a) indicates that there are ring-like products in plenty. And the high magnification FESEM image (Fig. 2b) shows that each ring is in the similar size with the average inner diameter and outer diameter of 170 and 870 nm, respectively.

Fig. 2c displays CuO products with mesoporous structure, which keep the similar shape as Cu<sub>2</sub>O<sub>4</sub>. The high magnification FESEM image (Fig. 2d) shows the ring-like CuO with the inner diameter and outer diameter of 200 and 900 nm, which is made of nanoparticles with the average diameters of 40 nm.

A series of parallel experiments were performed to investigate the influence of reaction time on the morphology of copper oxalate, which was checked with the FESEM as shown in Fig. 3. Fig. 3a is the image of discus-like products with refluxing time of 30 min: their diameter is in the range of 800–1000 nm, and the center of the product began to sink. When the reaction time was prolonged to 60 min, the center of the products sank ulteriorly, and some of the ring-like began to appear, as shown in Fig. 3b. After refluxing for 120 min, the discus-like products were converted to ring-like completely as shown in Fig. 2a. When the reaction proceeded for

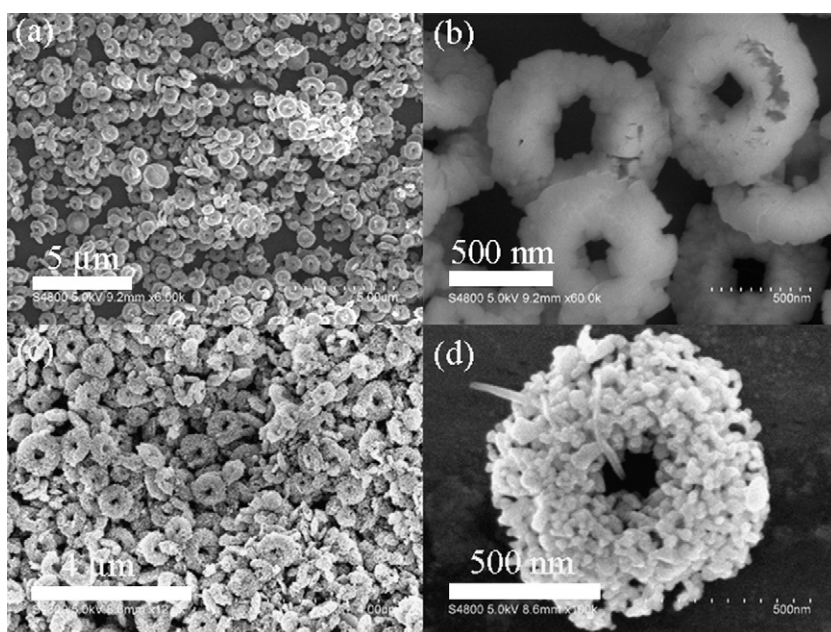
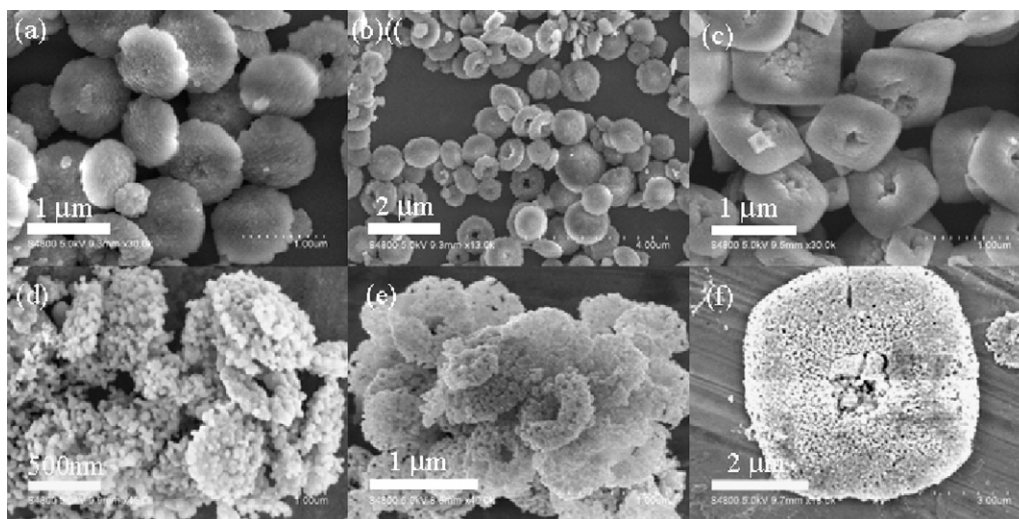
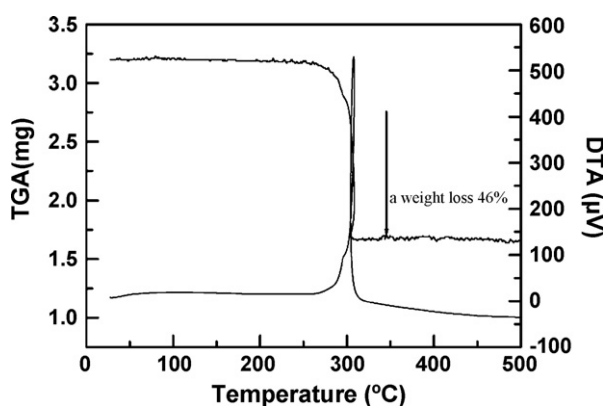


Fig. 2. FESEM images of the ring-like: (a) Cu<sub>2</sub>O<sub>4</sub> under low magnification, (b) Cu<sub>2</sub>O<sub>4</sub> under high magnification, (c) CuO under low magnification, and (d) CuO under high magnification.



**Fig. 3.** Time-dependent evolution of the ring-like morphology of the  $\text{Cu}_2\text{O}_4$  at different refluxing time: (a) 30 min, (b) 60 min, and (c) 180 min; And FESEM images of the CuO obtained by calcined the copper oxalate precursors with the refluxing time: (d) 30 min, (e) 60 min, and (f) 180 min.



**Fig. 4.** TGA and DSC curves of the copper oxalate precursors obtained with refluxing time of 120 min.

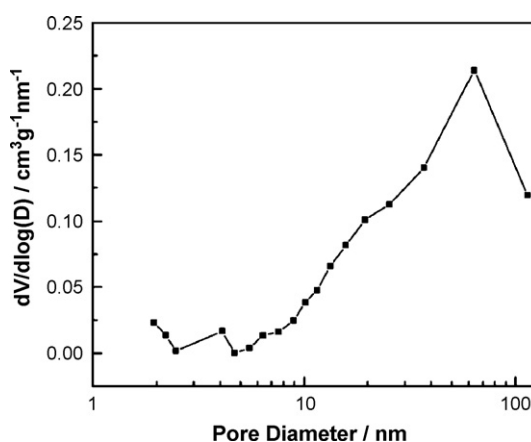


**Fig. 5.** The curve of the BJH pore-size distribution.

180 min, the morphology was changed greatly, as shown in Fig. 3c. Only the square  $\text{Cu}_2\text{O}_4$  with hole in the center was found, while the ring-like was disappeared. The side length of the square  $\text{Cu}_2\text{O}_4$  was ca. 800 nm. And the morphology and the size of the products kept unchanged with further increasing the refluxing time.

The corresponding copper oxalate precursors were calcined at 400 °C for 5 h. And Fig. 3d and e, and f show the SEM images of the CuO nanoparticles resulting from copper oxalate with different refluxing time (30, 60, and 180 min, respectively). All the images show that the nanostructures are also made up of CuO nanoparticles with the average diameter of 40 nm, which have high specific surface area and interspaces and may find applications in the fields of sensor and catalysis.

In the growth of copper oxalate, the  $\text{C}_2\text{O}_4^{2-}$  acts as a bidentate ligand in the aqueous solution to form the stable compound. It decreases the rate of the combining process and favors for controlling the morphology of the products as reported before [22], which is agreed with the brick-by-brick growth mechanism [21]. The direct role of the copper oxalate precursors is assuredly crucial, which serves as a template to form the CuO materials.

The TGA–DSC curves of the as-prepared precursors are shown in Fig. 4. There is a weight loss step in the temperature range of 290–310 °C, which may be ascribed to the decomposition of the oxalate. The weight loss is about 46.0%, which is close to the theoretical value [23].

The pore-size and distribution of the mesoporous CuO was measured on a Micrometrics ASAP-2000 adsorption apparatus (Fig. 5). The product of the mesoporous CuO has a wide porous diameter distribution with the central pore-size distribution of ca. 62 nm, which is probably caused by the two kinds of porous architecture in the products: one within the microspheres and the other from the interspaces of the constituent nanoparticles. And the surface area of the mesoporous CuO is 35.6  $\text{m}^2/\text{g}$ . Such mesoporous structure provides efficient transport pathways to their interior voids, which is critical for catalyst and other applications.

Fig. 6a shows the absorbance spectrum of the CuO materials, which exhibited prominent features at ca. 257 nm. An evaluation of the optical band gap is obtained using the following equation for a semiconductor:  $(\alpha) = A(h\nu/2 - E_g)^{m/2}$ , where  $A$  is a constant,  $\alpha$  is the absorption coefficient and  $m$  equals 1 for a direct transition. The energy intercept of a plot  $(\alpha E_{\text{plot}})^2$  vs.  $E_{\text{plot}}$  yields  $E_g$  for a direct transition (Fig. 6b). The band gap of the as-prepared CuO nanorings is calculated to be 3.43 eV from the UV–vis absorption spectrum, which is larger than the reported value for bulk CuO ( $E_g = 1.85$  eV) [24]. Presumably, this blue shift is explained by two combined factors: (1) the size of particles is in the intermediate confinement regime, where the size of particles is comparable to their Bohr exciton diameter and (2) spatial composition fluctuation can produce atomically abrupt jumps in the chemical potential, which

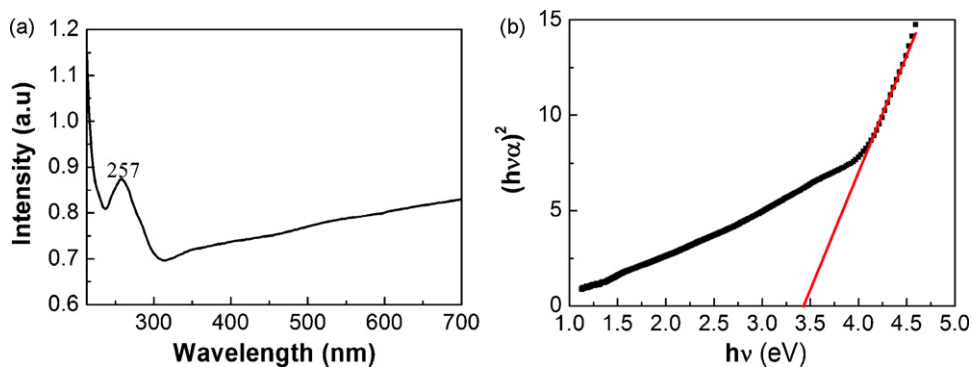


Fig. 6. (a) UV-vis absorption spectrum of the mesoporous CuO; (b) plot of the  $(\alpha E_{\text{plot}})^2$  vs.  $E_{\text{plot}}$  yields  $E_g$  for as-prepared mesoporous CuO.

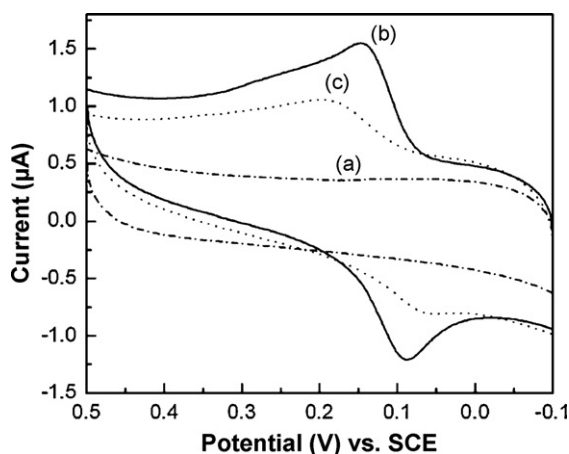


Fig. 7. CVs of  $1 \times 10^{-4}$  M DA in 0.1 M phosphate buffer solution (PBS pH 7.4) with scan rate of  $50 \text{ mV s}^{-1}$ : (a) CuO/GCE, (b) CuO/GCE and  $1.0 \times 10^{-4}$  M DA, and (c) bare GCE and  $1.0 \times 10^{-4}$  M DA.

localizes the free exciton states [25]. It might be reasonably speculated that the latter effect is more dominant in mesoporous copper oxide than the bulk CuO samples.

Fig. 7 shows the cyclic voltammograms of different electrodes in 0.01 M phosphate buffer solution (pH 7.4) at a scan rate of  $50 \text{ mV s}^{-1}$ . It shows no redox peak was observed with mesoporous CuO-modified GCE (curve a). While it using as the working electrode to detect  $1.0 \times 10^{-4}$  M dopamine (DA), a couple of distinct redox peaks were displayed (curve b), and the anodic and cathodic peak potentials are 145.6 and 88.36 mV, respectively, which has a negative direction shift for the anodic peak potential and positive shift for cathodic one comparing with the bare GCE (curve c). The separation between the peak potentials ( $\Delta E_p$ ) decreases from 121.8 to 57.24 mV, illustrating a more reversible system. In addition, the peak currents enhance remarkably. This phenomenon implies that the as-prepared products can improve the electron transfer between DA and the GC electrode. It should be ascribed to mesoporous morphology with high specific surface area, which results in a better reversibility in the electrochemical detection.

Because square-wave voltammogram (SWV) has a much higher sensitivity, it was employed to estimate the lower detection limit of DA. Fig. 8 shows the SWV recordings at various DA concentrations at the CuO/GCE in PBS (pH 7.4). A series of well-defined peaks are obtained owing to its good reversibility. After the correction of the background current, the detection limit of DA is calculated as  $1.0 \times 10^{-7}$  M, and the linear calibration graph (Fig. 8, inset) is obtained in the DA concentration range  $3.98 \times 10^{-6}$  to  $1.96 \times 10^{-4}$  M. The linear equation is calculated as  $i_{pa} = 0.3609 + 0.0054C_{DA}$  with the correlation coefficient of 0.9976.

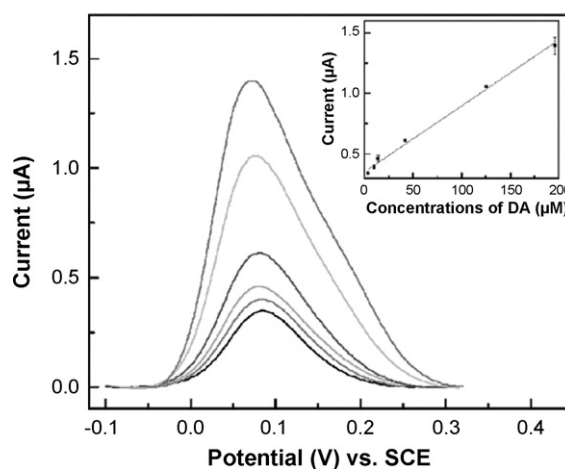


Fig. 8. SWV with CuO/GCE in a pH 7.4 phosphate buffer at different concentrations of DA: (a) 3.98  $\mu\text{M}$ , (b) 9.91  $\mu\text{M}$ , (c) 13.81  $\mu\text{M}$ , (d) 42.14  $\mu\text{M}$ , (e) 125.87  $\mu\text{M}$ , and (f) 196.10  $\mu\text{M}$ , and the linear plot of peak current vs. concentration of DA (inset).

#### 4. Conclusions

In summary, uniform, ring-like and high-purity CuO nanoparticles with the diameters of ca. 40 nm were successfully synthesized via a simple method using the copper oxalate as precursors. The refluxing time was found to have an influence on the morphology of the precursors. The obtained mesoporous CuO might find various potential applications in catalysis, electrochemistry, and optics because of the high specific surface area.

#### Acknowledgements

Financial support from the National Natural Science Foundation of China (20571001, 20675002), the Education Department (No. 2006KJ006TD) of Anhui Province and Anhui Provincial Natural Science Foundation (070414185) are appreciated.

#### References

- [1] H.L. Cao, Y. Wang, X.L. Yu, S.R. Wang, S.H. Wu, Z.Y. Yuan, Appl. Catal. B 79 (2008) 26.
- [2] S. Pavasupree, J. Jitputti, S. Ngamsinlapasathian, S. Yoshikawa, Mater. Res. Bull. 43 (2008) 149.
- [3] Y.G. Li, B. Tan, Y.Y. Wu, Nano Lett. 8 (2008) 265.
- [4] Y.Y. Xu, D.R. Chen, X.L. Jiao, K.Y. Xue, J. Phys. Chem. C 111 (2007) 16284.
- [5] J. Bao, Z.L. Liu, Y. Zhang, N. Tsubaki, Catal. Commun. 9 (2008) 913.
- [6] H. Li, H.L. Shi, H. Liang, X. Li, L. Li, M. Ruan, Mater. Lett. 62 (2008) 1410.
- [7] W.C. Geng, N. Li, X.T. Li, X.Y. Lai, L.F. Wang, B.H. Long, J.J. Ning, J.C. Tu, S.L. Qiu, Shilun, Mater. Res. Bull. 43 (2008) 601.
- [8] S. Tanaka, Y. Katayama, M.P. Tate, H.W. Hillhouse, Y. Miyake, J. Mater. Chem. 17 (2007) 3639.
- [9] M. Sivakumar, A. Gedanken, Z.Y. Zhong, L.W. Chen, New J. Chem. 30 (2006) 102.

- [10] Y.J. Zhang, Q.X. Hu, B. Hu, Z.Y. Fang, Y.T. Qian, Z.D. Zhang, *Mater. Chem. Phys.* 96 (2006) 16.
- [11] X.F. Yu, N.Z. Wu, Y. Xie, Y.Q. Tang, *J. Mater. Chem.* 10 (2000) 1629.
- [12] X.C. Jiang, T. Herricks, Y.N. Xia, *Nano Lett.* 2 (2002) 1333.
- [13] J.B. Reitz, E.I. Solomon, *J. Am. Chem. Soc.* 120 (1998) 11467.
- [14] H. Wang, J.Z. Xu, J.J. Zhu, H.Y. Chen, *J. Cryst. Growth* 244 (2002) 88.
- [15] P.E. de Jongh, D. Vanmaekelbergh, J.J. Kelly, *Chem. Commun.* (1999) 1069.
- [16] L.C. Soare, P. Bowen, J. Lemaitre, H. Hofmann, *J. Phys. Chem. B* 110 (2006) 17763.
- [17] S.S. Hayrapetyan, H.G. Khachatryan, *Micropor. Mesopor. Mater.* 89 (2006) 33.
- [18] B.V. L'Vov, *Thermochim. Acta* 364 (2000) 99.
- [19] M.A. Mohamed, A.K. Galwey, S.A. Halawy, *Thermochim. Acta* 429 (2004) 57.
- [20] A. Michalowicz, J.J. Girerd, J. Goulon, *Inorg. Chem.* 18 (1979) 3004.
- [21] N. Jongen, P. Bowen, J. Lemaitre, J.C. Valmalette, H. Hofmann, *J. Colloid Interface Sci.* 226 (2000) 189.
- [22] X.F. Zhao, J.G. Yu, *J. Cryst. Growth* 306 (2007) 366.
- [23] X.J. Zhang, D.E. Zhang, X.M. Ni, H.G. Zheng, *Solid-State Electron.* 52 (2008) 245.
- [24] K. Santra, C.K. Sarker, M.K. Mukherjee, B. Cosh, *Thin Solid Films* 213 (1992) 226.
- [25] H.K. Lee, H.S. Yang, P.H. Holloway, *J. Lumin.* 126 (2007) 314.